them have not been clinically observed long enough. In addition, the central reference flow cytometry laboratories of the JPLSG received samples and made immunophenotypic diagnoses even during the intervals between clinical studies. Therefore, in this study we did not concern ourselves with possible associations of antigen expression with the clinical, hematological or biological features, or attempt to determine the prognostic importance of antigen expression for the decision of treatments. Nevertheless, flow cytometric data generated by extensive use of our newly proposed immunological criteria together with common diagnostic panels developed according to the present analysis may be valuable for achieving more precise characterization of the leukemic blasts in each individual patient. This information, combined with the molecular and clinical features presented in the next standard clinical protocol for childhood ALL that will be issued by the JPLSG, will also contribute to the development of personalized medicine, the so-called tailor-made therapy, for each patient.

Acknowledgments We thank the committee members of the JPLSG for sending bone marrow and peripheral blood samples. This study was supported by a grant for Clinical Cancer Research from the Ministry of Health, Labor, and Welfare of Japan. We thank Dr. K. Nakahara, Ms. E. Ogawa and Mr. W. Hashimoto for their insightful and helpful comments.

References

1. Pui CH, Behm FG, Crist WM. Clinical and biologic relevance of immunologic marker studies in childhood acute lymphoblastic leukemia. Blood. 1993;82:343–62.
2. Borowitz MJ, Shuster J, Carroll AJ, Nash M, Look AT, Camitta B, et al. Prognostic significance of fluorescence intensity of surface marker expression in childhood B-precursor acute lymphoblastic leukemia. A Pediatric Oncology Group Study. Blood. 1997;89:3960–6.
3. Möricke A, Zimmermann M, Reiter A, Henze G, Schrauder A, Gadner H, et al. Long-term results of five consecutive trials in childhood acute lymphoblastic leukemia performed by the ALL-BFM study group from 1981 to 2000. Leukemia. 2010;24:265–84.
4. Escherich G, Horstmann MA, Zimmermann M, Janka-Schaub GE, COALL study group. Cooperative study group for childhood acute lymphoblastic leukaemia (COALL): long-term results of trials 82, 85, 89, 92 and 97. Leukemia. 2010;24:298–308.
5. Kamps WA, e Bruin KM, Veerman AJ, Fiocco M, Bierings M, Pieters R. Long-term results of Dutch Childhood Oncology Group studies for children with acute lymphoblastic leukemia from 1984 to 2004. Leukemia. 2010;24:309–19.
6. Schmiegelow K, Forestier E, Hellebostad M, Heyman M, Kristinsson J, Söderhäll S, et al. Long-term results of NOPHO ALL-92 and ALL-2000 studies of childhood acute lymphoblastic leukemia. Leukemia. 2010;24:345–54.
7. Pui CH, Pei D, Sandlund JT, Ribeiro RC, Rubnitz JE, Raimondi SC, et al. Long-term results of St Jude total therapy studies 11, 12, 13A, 13B, and 14 for childhood acute lymphoblastic leukemia. Leukemia. 2010;24:371–82.
8. Tsuchida M, Ohara A, Manabe A, Kumagai M, Shimada H, Kikuchi A, et al. Long-term results of Tokyo Children's Cancer Study Group trials for childhood acute lymphoblastic leukemia, 1984–1999. Leukemia. 2010;24:383–96.
9. Bene MC, Castoldi G, Knapp W, Ludwig WD, Matutes E, Orfao A, et al. Proposals for the immunological classification of acute leukemias. European Group for the immunological characterization of leukemias (EGIL). Leukemia. 1995;9:1783–6.
10. Campana D, Behm FG. Immunophenotyping of leukemia. J Immunol Methods. 2000;243:59–75.
11. Kaleem Z, Crawford E, Pathan MH, Jasper L, Covinsky MA, Johnson LR, et al. Flow cytometric analysis of acute leukemias. Diagnostic utility and critical analysis of data. Arch Pathol Lab Med. 2003;127:42–8.
12. Craig FE, Foon KA. Flow cytometric immunophenotyping for hematologic neoplasms. Blood. 2008;111:3941–67.
13. Coustan-Smith E, Mullighan CG, Onciu M, Behm FG, Raimondi SC, Pei D, et al. Early T-cell precursor leukaemia: a subtype of very high-risk acute lymphoblastic leukaemia. Lancet Oncol. 2009;10:147–56.
14. Vogler LB, Crist WM, Bockman DE, Pearl ER, Lawton AR, Cooper MD. Pre-B-cell leukemia. A new phenotype of childhood lymphoblastic leukemia. N Engl J Med. 1978;298:872–8.
15. Koehler M, Behm FG, Shuster J, Crist W, Borowitz M, Look AT, et al. Transitional pre-B-cell acute lymphoblastic leukemia of childhood is associated with favorable prognostic clinical features and an excellent outcome: a Pediatric Oncology Group study. Leukemia. 1993;7:2064–8.
16. Secker-Walker L, Stewart E, Norton J, Campana D, Thomas A, Hoffbrand V, et al. Multiple chromosome abnormalities in a drug resistant TdT positive B-cell leukemia. Leuk Res. 1987;11:155–61.
17. Walle AJ, Al-Katib A, Wong GY, Jhanwar SC, Chaganti RS, Koziner B. Multiparameter characterization of L3 leukemia cell populations. Leuk Res. 1987;11:73–83.
18. Shende A, Festa RS, Wedgwood JF, Lanzkowsky P. A paediatric case of a TdT positive B-cell acute lymphoblastic leukaemia (B-ALL) without Burkitt characteristics. Br J Haematol. 1988;70:129–30.
19. Finlay JL, Borcherding W. Acute B-lymphocytic leukemia with L1 morphology: a report of two pediatric cases. Leukemia. 1988;2:60–2.
20. Gluck WL, Bigner SH, Borowitz MJ, Brenckman WD Jr. Acute lymphoblastic leukemia of Burkitt's type (L3 ALL) with 8;22 and 14;18 translocations and absent surface immunoglobulins. Am J Clin Pathol. 1986;85:636–40.
21. Pui CH, Robison LL, Look AT. Acute lymphoblastic leukaemia. Lancet. 2008;371:1030–43.
22. Lai R, Juco J, Lee SF, Nahirniak S, Etches WS. Flow cytometric detection of CD79a expression in T-cell acute lymphoblastic leukemias. Am J Clin Pathol. 2000;113:823–30.
23. Bachir F, Bennani S, Lahjouji A, Cherkaoui S, Harif M, Khattab M, et al. Characterization of acute lymphoblastic leukemia subtypes in Moroccan children. Int J Pediatr. 2009;2009:674801.
24. Wiersma SR, Ortega J, Sobel E, Weinberg KI. Clinical importance of myeloid-antigen expression in acute lymphoblastic leukemia of childhood. N Engl J Med. 1991;324:800–8.
25. Pui CH, Shell MJ, Raimondi SC, Head DR, Rivera GK, Crist WM, et al. Myeloid antigen expression in childhood acute lymphoblastic leukemia. N Engl J Med. 1991;325:1378 (correspondence).
26. Borowitz MJ, Shuster JJ, Land VJ, Steuber CP, Pullen DJ, Vietti TJ. Myeloid antigen expression in childhood acute lymphoblastic leukemia. N Engl J Med. 1991;325:1378 (correspondence).
27. Reiter A, Schrappe M, Ludwig WD, Hiddemann W, Sauter S, Henze G, et al. Chemotherapy in 998 unselected childhood acute

lymphoblastic leukemia patients. Results and conclusions of the multicenter trial ALL-BFM 86. Blood. 1994;84:3122–33.
28. Uckun FM, Gaynon PS, Sensel MG, Nachman J, Trigg ME, Steinherz PG, et al. Clinical features and treatment outcome of childhood T-lineage acute lymphoblastic leukemia according to the apparent maturational stage of T-lineage leukemic blasts: a Children's Cancer Group study. J Clin Oncol. 1997;15:2214–21.
29. Putti MC, Rondelli R, Cocito MG, Aricó M, Sainati L, Conter V, et al. Expression of myeloid markers lacks prognostic impact in children treated for acute lymphoblastic leukemia: Italian experience in AIEOP-ALL 88–91 studies. Blood. 1998;92:795–801.
30. Bhatia S, Sather HN, Heerema NA, Trigg ME, Gaynon PS, Robison LL. Racial and ethnic differences in survival of children with acute lymphoblastic leukemia. Blood. 2002;100:1957–64.
31. Pui CH, Sandlund JT, Pei D, Rivera GK, Howard SC, Ribeiro RC, et al. Results of therapy for acute lymphoblastic leukemia in black and white children. JAMA. 2003;290:2001–7.
32. Kadan-Lottick NS, Ness KK, Bhatia S, Gurney JG. Survival variability by race and ethnicity in childhood acute lymphoblastic leukemia. JAMA. 2003;290:2008–14.

Sato et al. BMC Developmental Biology 2011, 11:22
http://www.biomedcentral.com/1471-213X/11/22

BMC Developmental Biology

RESEARCH ARTICLE Open Access

Lipid rafts enriched in monosialylGb5Cer carrying the stage-specific embryonic antigen-4 epitope are involved in development of mouse preimplantation embryos at cleavage stage

Ban Sato[1,4], Yohko U Katagiri[1*], Kenji Miyado[2], Nozomu Okino[3], Makoto Ito[3], Hidenori Akutsu[2], Hajime Okita[1], Akihiro Umezawa[2], Junichiro Fujimoto[1], Kiyotaka Toshimori[4] and Nobutaka Kiyokawa[1]

Abstract

Background: Lipid rafts enriched in glycosphingolipids (GSLs), cholesterol and signaling molecules play an essential role not only for signal transduction started by ligand binding, but for intracellular events such as organization of actin, intracellular traffic and cell polarity, but their functions in cleavage division of preimplantation embryos are not well known.

Results: Here we show that monosialylGb5Cer (MSGb5Cer)-enriched raft domains are involved in development during the cleavage stage of mouse preimplantation embryos. MSGb5Cer preferentially localizes at the interfaces between blastomeres in mouse preimplantation embryos. Live-imaging analysis revealed that MSGb5Cer localizes in cleavage furrows during cytokinesis, and that by accumulating at the interfaces, it thickens them. Depletion of cholesterol from the cell membrane with methyl-beta-cyclodextrin (MbCD) reduced the expression of MSGb5Cer and stopped cleavage. Extensive accumulation of MSGb5Cer at the interfaces by cross-linking with anti-MSGb5Cer Mab (6E2) caused F-actin to aggregate at the interfaces and suppressed the localization of E-cadherin at the interfaces, which resulted in the cessation of cleavage. In addition, suppression of actin polymerization with cytochalasin D (CCD) decreased the accumulation of MSGb5Cer at the interfaces. In E-cadherin-targeted embryos, the MSGb5Cer-enriched raft membrane domains accumulated heterotopically.

Conclusions: These results indicate that MSGb5Cer-enriched raft membrane domains participate in cytokinesis in a close cooperation with the cortical actin network and the distribution of E-cadherin.

Background

The molecular dynamics involved in embryogenesis is now being elucidated. In the early cleavage stage of embryogenesis, the localization of cell surface molecules periodically changes and is spatio-temporally controlled. Cytokinesis is a fundamental process of cell cleavage in which the daughter cells split after nuclear division, and it is driven by actin-dependent narrowing of a contractile ring as well as furrow-specific addition of membrane [1,2]. The latter contributes to dynamic rearrangement of cell surface proteins and provides molecules required to construct the complex machinery of cytokinesis. For example, the cell surface adhesion molecule E-cadherin is drastically rearranged in a close correlation with the dynamics of cortical actin [3]. It is well documented that E-cadherin is located predominantly in membrane domains involved in cell-cell contacts of adjacent blastomeres and mediates adhesion between blastomeres of preimplantation mouse embryos from 8-cell stage onwards [4-6].

A new aspect of the cell membrane structures called "lipid rafts" has been postulated [7]. Lipid rafts have been described by Lingwood and Simons as "fluctuating nanoscale assemblies of sphingolipid, cholesterol, and proteins that can be stabilized to coalesce into platforms

* Correspondence: kata@nch.go.jp
[1]Department of Pediatric Hematology and Oncology Research, National Research Institute for Child Health and Development, 2-10-1 Okura, Setagaya-ku, Tokyo 157-8535, Japan
Full list of author information is available at the end of the article

that function in membrane signaling and trafficking" [8]. During cell cleavage in embryogenesis, lipid rafts were shown to play an essential role in central spindle assembly and cleavage furrow ingression [1]. For example, GM1 is a monosialylated ganglio-series glycosphingolipid (GSL), which is most commonly used as a raft marker. The lipid rafts enriched in GM1 at the cleavage furrow were shown to possess signaling machinery that contributes to cytokinesis during the cleavage of sea urchin eggs and mouse preimplantation embryos [9,10].

We recently reported finding that monoclonal antibody (Mab) 6E2 raised against human embryonal carcinoma cell line recognizes the globo-series GSL MSGb5Cer is present at the interfaces between blastomeres of living mouse embryos [11]. MSGb5Cer carries an epitope of stage-specific embryonic antigen-4 (SSEA-4), which expressed only in the early cleavage stage of mouse embryos. Lipid rafts enriched with MSGb5Cer was also reported to interact with E-cadherin in breast cancer cell lines [12]. Therefore, MSGb5Cer is expected to form lipid rafts on mouse preimplantation embryos and play an important role in the process of cleavage division. To elucidate the functional role of MSGb5Cer enriched-lipid rafts in embryogenesis, in this study we investigated the dynamics of MSGb5Cer in preimplantation embryos during the course of early embryonic cleavage.

Results

MSGb5Cer and E-cadherin localize at the interfaces between the blastomeres in mouse preimplantation embryos

MSGb5Cer, E-cadherin, and GM1 were visualized in living mouse preimplantation embryos, and their localizations are shown in the optical slice images in Figure 1A. MSGb5Cer and E-cadherin were stained with Mabs 6E2 and ECCD-2, respectively, and they were localized on the cell surface in dotted form in unfertilized eggs but excluded from the area over the meiotic spindle. GM1, on the other hand, was stained with the cholera toxin B subunit (CTX-B) and had accumulated in a perivitelline space in unfertilized eggs, and its accumulation accelerated after fertilization. Preferential localization of MSGb5Cer and E-cadherin at interfaces between blastomeres was also observed in compacted 8-cell stage embryos, whereas GM1 mainly localized at the outer surface area and only a small amount of GM1 was detected at the interfaces. A part of MSGb5Cer was localized similar to GM1 at the outer surface area of blastomeres. These results indicate that MSGb5Cer and E-cadherin, but not GM1, are similarly distributed in preimplantation embryos.

Next, we enzymatically prepared fluorescence-labeled MSGb5Cer or GM1 and introduced into embryos instead of staining with GSL-specific Mab 6E2 or ligand CTX-B to visualize GSLs on embryos. As shown in the optical slice images in Figure 1B, BODIPY®FL-MSGb5Cer was distributed mainly at the interfaces between blastomeres, whereas BODIPY®FL-GM1 was evenly distributed over the surface and in the perivitelline space. In contrast, BODIPY®FL-C12 fatty acids, as a negative control, were not detected at all. The results coincided with that shown by immunostaining. The prolonged culture of BODIPY®FL-MSGb5Cer-introduced embryo in the presence of 6E2 at the same concentration used for immunostaining in Figure 1A did not affect preferential localization of MSGb5Cer, or did not induce the aggregation of MSGb5Cer (Figure 1C). Therefore, it is indicated that the preferential localization of MSGb5Cer at interfaces is due to spontaneous accumulation of MSGb5Cer at interfaces and is not due to the artifactual aggregation of MSGb5Cer induced by cross-linking with antibody.

MSGb5Cer accumulates in the cleavage furrow of preimplantation embryos during cytokinesis, and then at the interfaces after cytokinesis

Time-lapse images of MSGb5Cer visualized with MSGb5Cer-specific Mab (6E2) are shown in Figure 2A. MSGb5Cer began to accumulate at the site of the future furrow (indicated by the arrow) of the spherical zygote at 150 minutes, and accumulation later accelerated and peaked at 180 minutes. Accumulation at the interface also accelerated, and after peaking at 240 minutes, gradually decreased to the initial level at 360 minutes (Figure 2A, B; see the Movie in additional file 1). The means ± s. d. of the fluorescence intensities in the furrow and at the interface of 6 embryos in the round stage, during cytokinesis, after cytokinesis, and in the late 2-cell stage are shown in Figure 2C. MSGb5Cer accumulated in the furrow at the start of cytokinesis and moved to the interface as cytokinesis proceeded. After cytokinesis, the accumulation was gradually broken, and MSGb5Cer eventually became evenly distributed over the entire cell surface, including the interface.

Overlapping distribution of MSGb5Cer with cholesterol

Cholesterol is known to be an important constituent of lipid rafts. Since MSGb5Cer is thought to be also involved in the formation of raft membrane domains in preimplantation embryos, we examined the distribution of cholesterol with Filipin III in the 6E2-stained and fixed embryos. The merged images of MSGb5Cer and cholesterol showed overlapping localization at the interfaces between blastomeres (Figure 3).

MbCD causes de-compaction and subsequent suppression of cell division

Since cholesterol has been postulated to be an absolute requirement for raft integrity, MbCD, which depletes

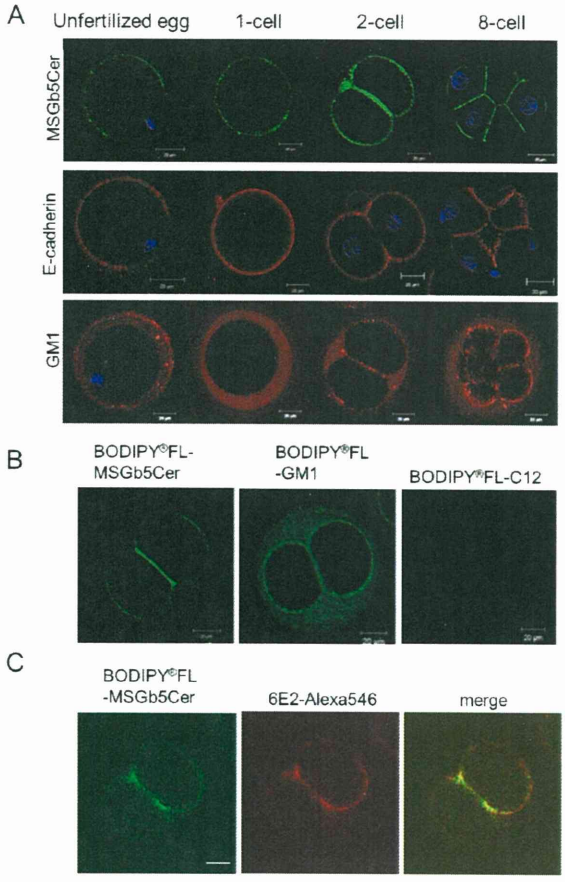

Figure 1 MSGb5Cer localize at the interfaces between blastomeres in mouse preimplantation embryos. (A) Localization of MSGb5Cer, E-cadherin and GM1 in an unfertilized egg and an embryo at the zygote, 2-cell stage and 8-cell stage. MSGb5Cer (top row), E-cadherin (middle row), and GM1 (bottom row) in a living mouse egg or embryos were stained with Alexa Fluor® 488-conjugated 6E2, ECCD-2/Alexa Fluor® 546 Rabbit Anti-rat IgG, and biotinylated-CTX B/Alexa Fluor® 546 streptavidin, respectively, and examined. Thirty sample unfertilized egg and 45 sample embryos of other stages were used for this experiment represented in image. (B) Distribution of BODIPY®FL-MSGb5Cer and BODIPY®FL-GM1 in a 2-cell stage embryo. The distribution of MSGb5Cer and GM1 is shown in the form of optical slice images. BODIPY®FL-C12 fatty acid was used as a negative control. All scale bars represent 20 μm. Ten sample 2-cell stage embryos were used for this experiment represented in each image. (C) Distribution of BODIPY®FL-MSGb5Cer in a 2-cell stage embryo cultured in the presence of 6E2. The BODIPY®FL-MSGb5Cer introduced 2-cell embryo was cultured for 1 hour in M16 medium containing 15 μg/ml of 6E2, and then stained with Alexa Fluor® 546-conjugated 6E2. Scale bar represent 20 μm. Ten sample 2-cell stage embryos were used for this experiment represented in image.

cholesterol from the cell surface, has been used as a tool in lipid raft research [13-15]. To investigate the correlation between raft integrity and the distribution of MSGb5Cer, GM1, and E-cadherin in the embryos, compacted 8-cell embryos were pretreated with various concentrations of MbCD for 15 minutes and then examined. As shown in Figure 4A, pretreatment of the embryos with 0.5 mM MbCD induced decompaction and decreased expression of MSGb5Cer at the interface between blastomeres. The expression on the outer membrane of blastomeres was not decreased and rather seemed to be increased. At a higher concentration (5 mM), expression of MSGb5Cer on the cell surface was further reduced, whereas expression of GM1 and E-cadherin was unaffected. The green fluorescence signals detected in the zona pellucida of 5 mM MbCD-treated embryos are thought to be derived from MSGb5Cer released from the embryo. Treatment with 10 mM MbCD caused complete loss of MSGb5Cer, and decreased expression of GM1, but there were no change in E-cadherin expression.

Next, we investigated the importance of raft integrity in viability of embryos. Pretreatment of 8-cell embryos with MbCD suppressed normal development in a time- and concentration-dependent manner (Figure 4B, C). All embryos in the control culture survived and developed normally into blastocysts by 48 hours of culture, whereas none of embryos pretreated with 0.5 mM MbCD had survived

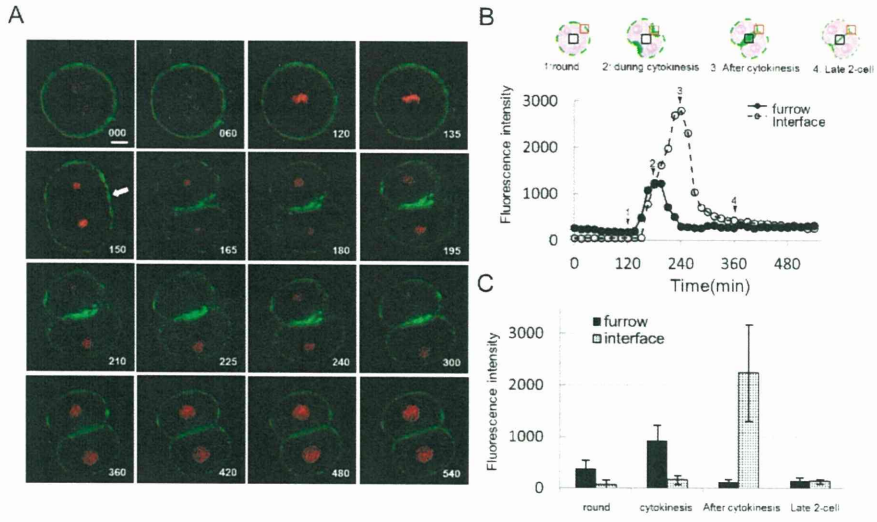

Figure 2 MSGb5Cer accumulates at the interface during cytokinesis in preimplantation embryos. (A) Frames from a series of confocal time-lapse movies of live cytokinesis-stage cells stained with 6E2 for MSGb5cer (green) and with DAPI for nuclei (red). Frames are shown at 60-minute intervals from 0 to 120 minutes, 15-minute intervals from 120 minutes to 240 minutes, and 60-minute intervals from 240 minutes to 540 minutes. Time is expressed in minutes after the start of culture. The arrow at 150 minutes points to the site of a future furrow in the spherical zygote. Scale bar represents 20 μm. The images shown are representative of nine sample zygotes. (B) Temporal changes in fluorescence intensity at the furrow and the interface region during cytokinesis. The fluorescence intensity in pixel values was measured in boxes of equal size located at the furrow (red square) and the interface (black square) of the frames taken every 15 minutes from a confocal time-lapse movie of the zygote of Figure 2A. The fluorescence intensity values at the furrows (closed circles) and interface (open circles) were plotted against time in minutes. Schematic embryos at the round stage (1), during cytokinesis (2), after cytokinesis (3), and the late 2-cell stage (4) were cultured for 105 minutes, 165 minutes, 240 minutes, and 405 minutes, respectively. This data shown is representative of nine sample zygotes. (C) The fluorescence intensity of MSGb5Cer at the furrow (closed column) and interface (dotted column) in round, cytokinesis, post-cytokinesis and late 2-cell stage embryos. Mean values and s.d. were calculated from the results obtained from the time-lapse movies of 6 embryos shown in Figure 2B.

by 48 hours of culture. These results suggest that MSGb5Cer is more sensitive than GM1 to raft integrity, and that lipid raft is prerequisite to cell adhesion and normal development of preimplantation embryos.

Extensive accumulation of MSGb5Cer to interfaces is related to delay and suppression of normal development

As shown in Figure 5A, incubation for 1 hour in the presence of 100 μg/ml of anti- MSGb5Cer Mab 6E2, but not of the isotype-matched control Mab 15B2, led to extensive accumulation of MSGb5Cer at the interfaces in the embryos, and a large aggregate of BODIPY® FL-MSGb5Cer was found.

Prolonged culture of 2-cell embryos in the presence of 6E2 caused a decrease in survival rate, and more than 90% of the embryos died before developing into blastocysts (Figure 5B). 80% of embryos were died after 12 hour culture in 6E2, whereas all of embryos cultured in control Mabs were alive. After 24 hour-culture, embryos cultured in 6E2 cleaved abnormally, and their cleavage rate was delayed as compared with those cultured in control Mabs. The morula embryo, which was able to avoid being injured, seemed to be compacted (arrow in 48 hour culture in 6E2). The anti-MSGb5Cer Mab 6E2 we used in this study is not toxic and do not have non-specific effects on preimplantation embryos, because 100 μg/ml of 6E2 antibody does not affect viability of blastocyst stage embryos that no longer express MSGb5Cer (see Figure S1 in additional file 2). In addition, when either the isotype-matched control Mab 15B2 or anti-E-cadherin Mab ECCD-2 was similarly tested, they did not affect viability of embryos (Figure 5).

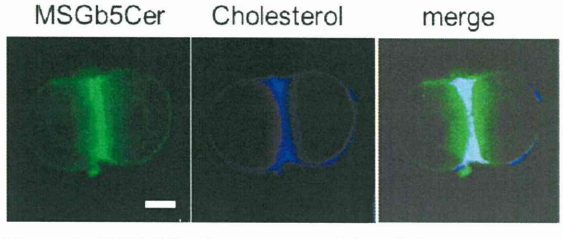

Figure 3 MSGb5Cer is overlapped by cholesterol at the interface in a 2-cell embryo. A two-cell stage embryo was stained with 6E2 for MSGb5cer (green) and then filipin III for cholesterol (blue) as described in Materials and Methods. Scale bar: 20 μm. Ten sample 2-cell stage embryos were used for this experiment represented in images.

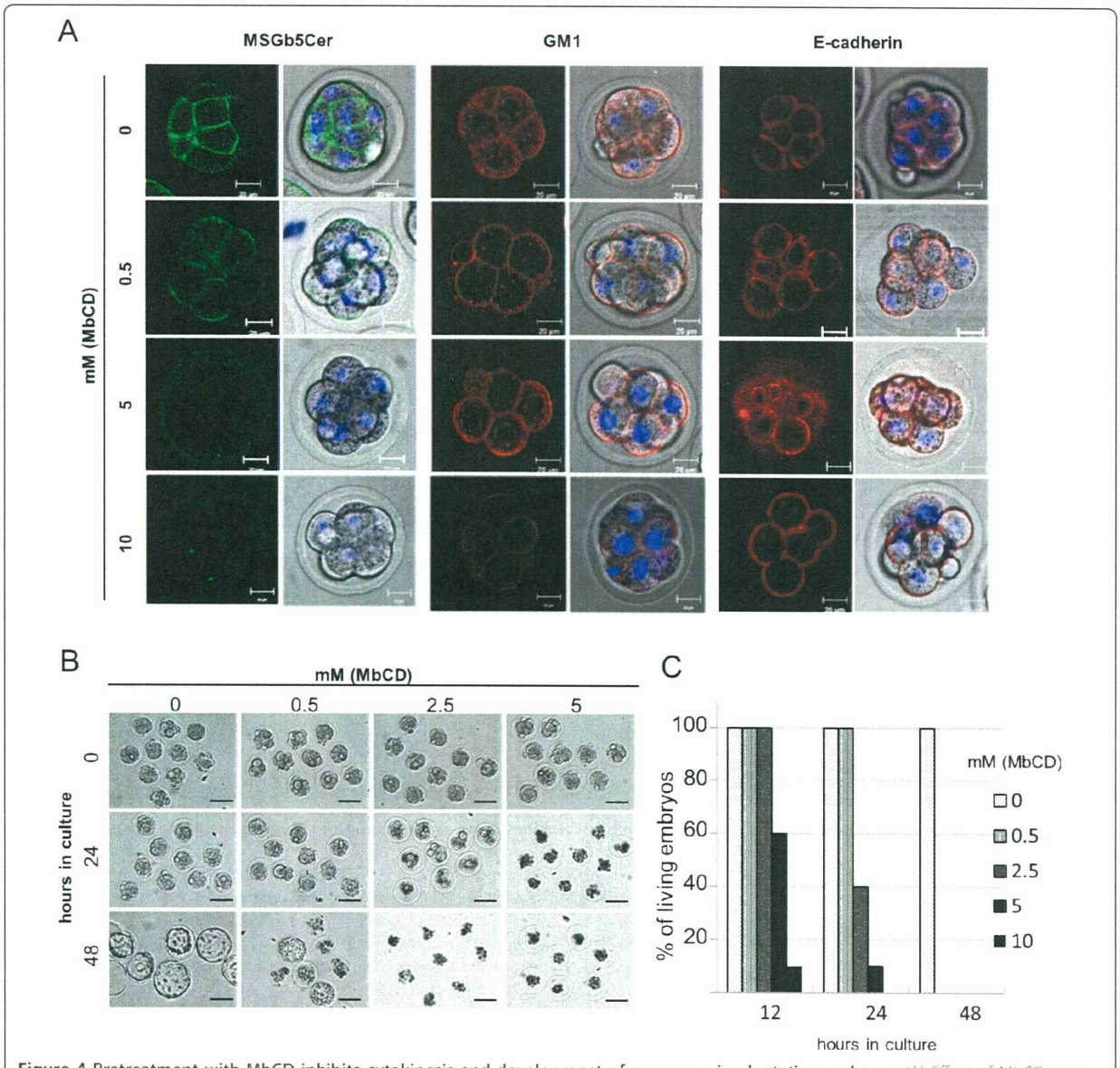

Figure 4 Pretreatment with MbCD inhibits cytokinesis and development of mouse preimplantation embryos. (A) Effect of MbCD on the expression of MSGb5Cer (green), GM1 (red) and E-cadherin (red) on 8-cell embryos. The left column and the right column of each panel represent a 2D image and the overlay of a 2D image and a differential interference contrast (DIC) micrograph, respectively. Thirty 8-cell embryos were used for the experiment represented in the images. (B) Representative DIC images of embryos cultured for 0, 24 and 48 hours in M16 medium after preincubation with 0-5 mM MbCD. Scale bars: 100 μm. Twenty 8-cell embryos were used for the experiment represented each images. (C) The percentages of living embryos cultured for 12, 24 and 48 hours after preincubation with 0-5 mM MbCD. Twenty 8-cell embryos were cultured for each concentration of MbCD.

In the 2-cell embryos cultured for 2 hours with 6E2, a large amount of F-actin accumulated at the interfaces, whereas no E-cadherin was detected at the interfaces, and it almost localized on the outer surface of blastomeres (Figure 5C). The entry of E-cadherin into the interfaces in living embryos was inhibited after treatment with Mab 6E2 in a dose-dependent manner (Figure 5D).

MSGb5Cer did not accumulate at the interfaces in actin-depolymerized 2-cell embryos

Actin filaments are thought to generate a mechanical force that drives membrane molecules or domains during cytokinesis. We investigated the effect of disruption of actin filaments with CCD on the localization of MSGb5Cer. As shown in Figure 6, when 2-cell stage embryos preincubated with 0, 0.2, and 2 μg/ml of CCD

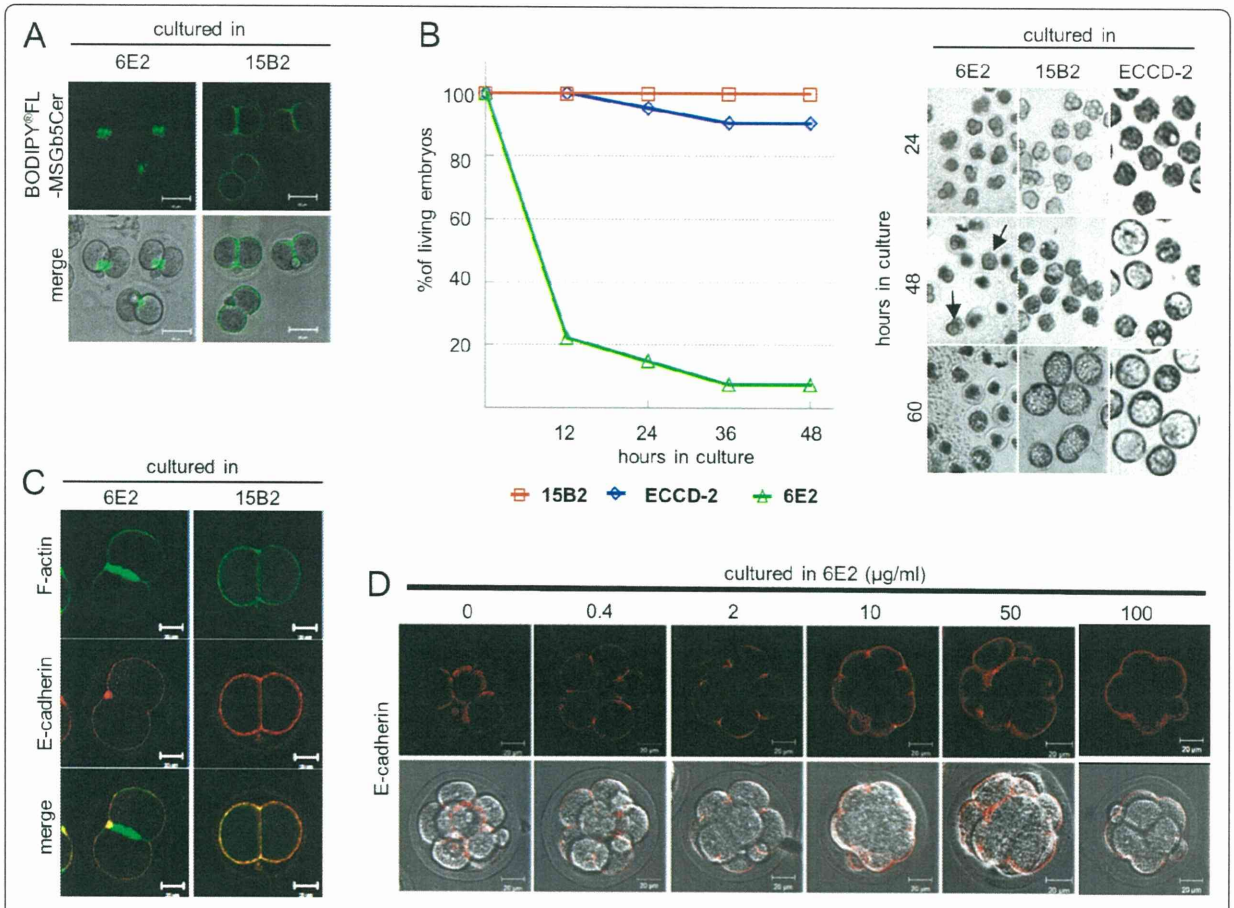

Figure 5 Extensive cross-linking of MSGb5Cer with 6E2 inhibits cytokinesis and development of mouse preimplantation embryos (A) Deposition of BODIPY®FL-MSGb5Cer at the interfaces of 2-cell stage embryos cultured in the presence of 6E2. Embryos labeled with BODIPY®FL-MSGb5Cer (green) were cultured for 1 hour in M16 medium containing 100 μg/ml of 6E2 or 15B2 antibodies. A fluorescence 2D image of BODIPY®FL-MSGb5Cer and the overlay of a 2D image and DIC micrograph of cultured embryos are shown. These images shown are representative of twelve 2-cell embryos. (B) Effect of cross-linking of MSGb5Cer with 6E2 on cytokinesis and the development of mouse preimplantation embryos. Two-cell embryos were cultured for 60 hours in M16 medium containing 100 μg/ml of 15B2 (red squares), ECCD-2 (blue diamonds), and 6E2 (green triangles), and the living embryos were counted and their DIC images were taken at the times indicated. Arrows indicate compacted embryos. Twenty of 2-cell stage embryos were cultured for each experiment groups. (C) Localization of F-actin and E-cadherin in MSGb5Cer-cross-linked 2-cell embryos. Two-cell embryos treated for 2 hours with 6E2 (left column) or 15B2 (right column) were fixed and stained with Alexa Fluor® 633 phalloidin and anti E-cadherin/Alexa Fluor® 546-conjugated rabbit anti-rat IgG. These images shown are representative of twelve 2-cell embryos. (D) Inhibitory effect of cross-linking of MSGb5Cer with 6E2 on the localization of E-cadherin at interfaces. Embryos were immunostained with ECCD-2/Alexa Fluor® 546-conjugated Rabbit Anti-rat IgG (red) in the presence of various concentrations of 6E2. The upper row and the bottom row of each panel represent a 2D image and the overlay of a 2D image and DIC micrograph, respectively. These images shown are representative of thirty morula embryos.

were immunostained with anti-MSGb5Cer Mab 6E2, accumulation of MSGb5Cer at the interface was suppressed in a dose-dependent manner. These results suggest that inhibition of F-actin polymerization by CCD prevents the localization of MSGb5Cer at the interface.

Absence of E-cadherin causes heterotopic localization of MSGb5Cer on the blastomere surface

To investigate the involvement of E-cadherin in the localization of MSGb5Cer at the interface, we generated embryos lacking maternal E-cadherin, and examined them. In control 2-cell embryos (Genotype; Floxed/+), MSGb5Cer and E-cadherin exhibited a similar distribution pattern and accumulated at the interface (Figure 7 upper row). In E-cadherin null mutant 2-cell embryos (Genotype; Floxed del/+), adhesion between the blastomeres was weaker and the area of the interface plane was greatly reduced (Figure 7 middle and bottom row). In these embryos, MSGb5Cer formed heterotopic aggregates (indicated by the arrow) or assembled at the outer

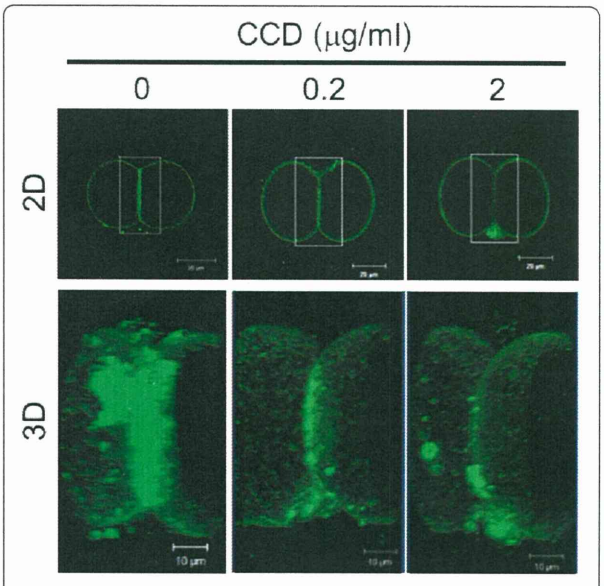

Figure 6 Disruption of actin filaments suppresses localization of MSGb5Cer at the interface. Two-cell embryos pretreated with 0, 0.2, and 2 μg/ml of CCD were immunostained with Alexa Fluor® 488-conjugated 6E2 (green). The 3D images were constructed by stacking optical slice images of the area enclosed by the square. Scale bar: 20 μm (2D), 10 μm (3D). These images shown are representative of thirty 2-cell stage embryos.

surface membranes of the blastomeres (indicated by the arrowhead). These results suggest that E-cadherin is required not for assembly, but for localization of MSGb5Cer at the interface of blastomeres.

Discussion and Conclusions

In this study, we investigated the involvement of MSGb5Cer in the development of mouse preimplantation embryos. As presented in Figure 2, MSGb5Cer moved to the future site of the cleavage furrow and accumulated at the interfaces between blastomeres as cytokinesis proceeds during embryonic development of mouse preimplantation embryos. Once, however, cytokinesis is complete the MSGb5Cer have accumulated at the interfaces evenly redistribute themselves over the cell surface (Figure 2).

MSGb5Cer is thought to be involved in the formation of raft membrane domains. Indeed, we observed overlapped localization of MSGb5Cer and cholesterol, an important constituent of lipid rafts (Figure 3). The finding that disruption of the integrity of lipid rafts by removal of cholesterol from the cell membrane with MbCD caused the release of MSGb5Cer into the perivitelline space (Figure 4) should further support above notion. Interestingly, as we presented in this study (Figure 1), GM1 and MSGb5Cer localize differently, suggesting that they may belong to different lipid rafts that possess distinct functions as described in several studies [16-18].

Since GM1 is easily detected with CTX-B, it is considered one of the most important marker GSLs for lipid rafts. Comiskey and Warner reported observation that GM1 visualized with biotinylated CTX-B were enriched at the cleavage furrow in mouse 2-cell and 4-cell embryos which actively undergo cytokinesis [10]. Burgess DR and his co-workers also reported that plasma membrane domains enriched in GM1 contain signalling machinery that contributes to cytokinesis and accumulate in the equatorial plasma membrane at mid-anaphase in sea urchin eggs [9], and further revealed that cells are polarized upon insertion of distinct basolateral membrane at the first division using the apical marker GM1 and the aPKC-PAR6 complex [19]. Although GM1 is constantly expressed throughout the cleavage stage in preimplantation embryos, MSGb5Cer is expressed only in the early cleavage stage from the unfertilized egg stage to morula stage embryos and more abundantly enriched at the cleavage furrow than GM1 during the course of cytokinesis (Figure 1). MSGb5Cer should therefore play a more specific role as a constituent of lipid rafts at this stage.

As described above, MbCD-mediated disruption of the integrity of lipid rafts caused the release of MSGb5Cer into the perivitelline space and decompaction of compacted 8-cell embryos and suppressed cell division. Comiskey and Warner also showed that cholesterol depletion by treatment of zygotes with MbCD inhibits preimplantation development from zygotes to blastocysts stage in culture in a dose-dependent manner [10]. On the other hand, heavy cross-linking of MSGb5Cer with MSGb5Cer-specific Mab induces extensive aggregation of MSGb5Cer (Figure 5) and suppressed cytokinesis. As a consequence, normal embryonic development would be terminated in both cases. Therefore, lipid rafts enriched in MSGb5Cer should play an important role in cytokinesis as well as in embryogenesis.

During cytokinesis, the cortical actin network form a scaffold for membrane proteins and thereby transfer them toward the cleavage furrow [3]. E-cadherin knockout mice display embryonic lethality and embryos are unable to form adhesion complexes [20,21]. In this study, we also presented close correlations between lipid rafts enriched in MSGb5Cer and E-cadherin as well as the cortical actin network. In preimplantation embryos, MSGb5Cer and E-cadherin are similarly distributed at the interfaces between blastomeres in 8-cell embryos, while MbCD-treatment caused the release of MSGb5Cer into the perivitelline space, decompaction of compacted embryos and even distribution of E-cadherin on the cell surface. In 2-cell embryos lacking E-cadherin, however, the MSGb5Cer-enriched lipid rafts accumulated

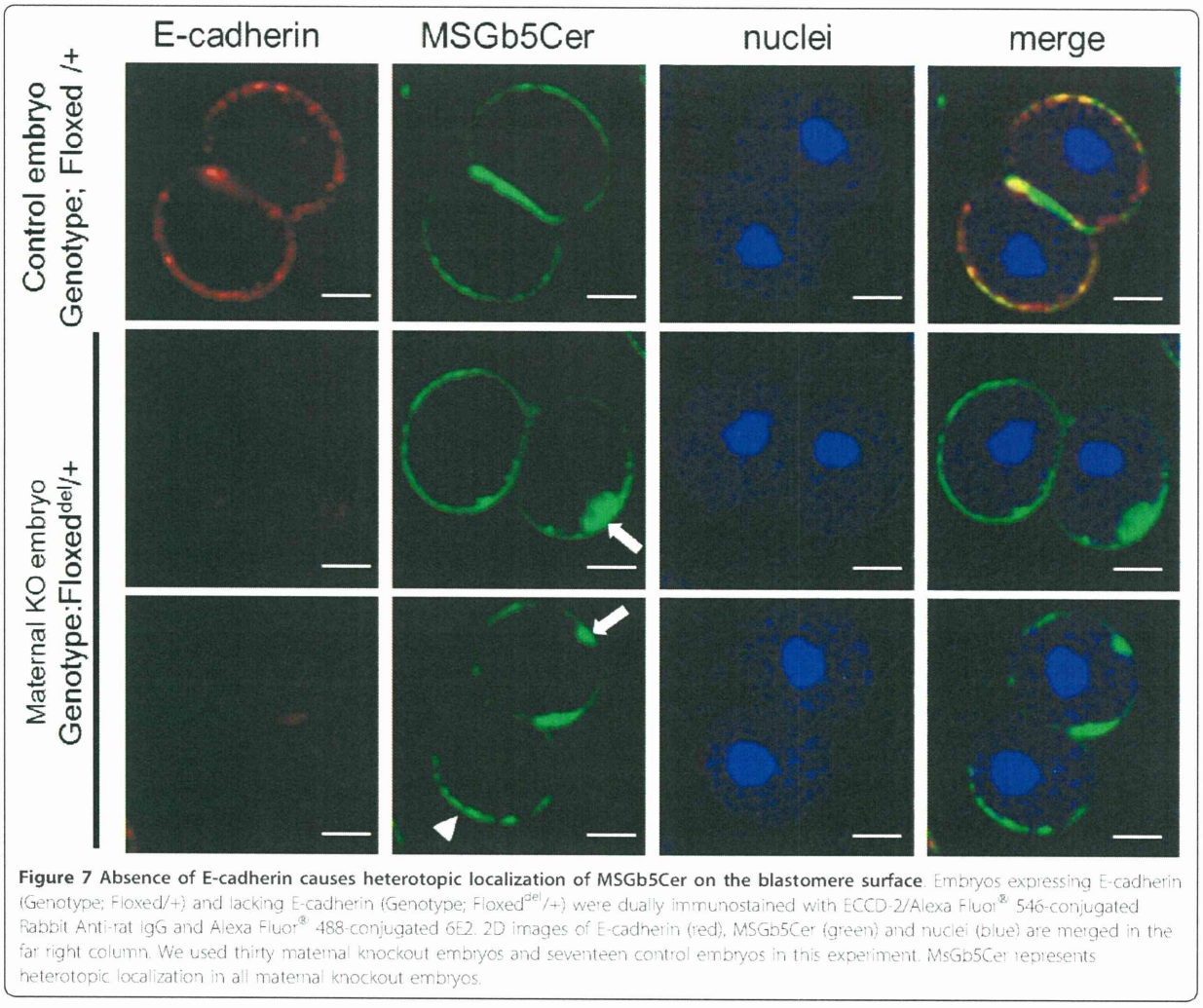

Figure 7 Absence of E-cadherin causes heterotopic localization of MSGb5Cer on the blastomere surface. Embryos expressing E-cadherin (Genotype; Floxed/+) and lacking E-cadherin (Genotype; Floxed^{del}/+) were dually immunostained with ECCD-2/Alexa Fluor® 546-conjugated Rabbit Anti-rat IgG and Alexa Fluor® 488-conjugated 6E2. 2D images of E-cadherin (red), MSGb5Cer (green) and nuclei (blue) are merged in the far right column. We used thirty maternal knockout embryos and seventeen control embryos in this experiment. MsGb5Cer represents heterotopic localization in all maternal knockout embryos.

heterotopically at sites other than the interface, indicating a close association with E-cadherin in maintaining the integrity of MSGb5Cer movement. On the other hand, disruption of polymerization of F-actin with CCD dose-dependently inhibited accumulation of MSGb5Cer at the interfaces, suggesting that the movement of MSGb5Cer-enriched lipid rafts into interfaces is driven by F-actin. During extensive aggregation of MSGb5Cer induced by cross-linking with specific antibody, all of the F-actin accumulated at the interfaces.

Although the details are still remaining to be clarified and further experiments are clearly needed, these results suggest that MSGb5Cer-enriched lipid rafts are driven into the furrow by the cortical actin network in close association with E-cadherin and play a role in cytokinesis in the early cleavage stage of mouse preimplantation embryos and our findings in this study should provide clues to the functional role of lipid rafts in early embryogenesis.

Methods

Embryo collection and culture

In all experiments, 6-8 week old female BDF1 mice purchased from CLEA Japan. Inc. (Tokyo, Japan) were induced to superovulated by intraperitoneal injections of pregnant mares' serum (ASKA Pharmaceutical Co., Ltd., Japan), and of human chorionic gonadotropin (hCG; ASKA Pharmaceutical Co., Ltd.) 48 hours later. Immediately after the hCG injection, each female mouse was mated with a male of the same strains. Zygotes and 2-cell and 8-cell embryos were collected by flushing out of the oviducts into M16 medium at 24 hours, 36 hours, and 60 hours, respectively, after the hCG injection and then cultured at 37°C in a conventional incubator. Animals were treated according to the institutional animal care and use guidelines of the National Research Institute for Child Health and Development. To obtain embryos lacking maternal E-cadherin, C57BL/6 mice were crossed as shown in Figure S2 in additional file 3

according to the procedure described by De Vries et al. [21]. The embryos did not express E-cadherin translated from paternal transcripts, at least until the 2-cell stage. Genotyping of all mice was performed by PCR using DNA extracted from ear snips of 28-day-old mice with an Automatic DNA Extraction System (NA-3000, KURABO, Tokyo, Japan). The following primer pair specific for cre recombinase was used to determine whether the Zp3-cre transgene was present: Cre1 (5'-ATG CCC AAG AAG AAG AGG AAG GT-3'), Cre2 (5'-GAA ATC AGT GCG TTC GAA CGC TAG A-3'). The primer pairs used to detect the different alleles of E-cadherin were as described previously by Boussadia et al. [22].

Antibodies and chemicals

Alexa Fluor® 488-conjugated 6E2, used for staining MSGb5Cer, was prepared as previously described [11]. Anti-mouse E-cadherin Mab ECCD-2 was purchased from TAKARA Bio. Co. (Tokyo Japan). Mab 15B2 was a generous gift of Dr. Taketo Yamada of Keio University School of Medicine [23]. Alexa Fluor® 633 phalloidin and Alexa Fluor® 546 CTX-B, used for staining actin and GM1, respectively, were purchased from Invitrogen. Alexa Fluor® 546 Rabbit Anti-rat IgG and Alexa Fluor® 546 streptavidin were also purchased from Invitrogen. Biotinylated-CTX-B of Sigma-Aldrich Inc. (St. Louis. MO) was also used. Filipin III, used for staining cholesterol, was purchased from Cayman Chem. Co. (Ann Arbor, MI). MbCD and CCD were obtained from Sigma and Calbiochem, respectively. GM1 and a monosialylganglioside mixture were purchased from Matreya Inc. (Pleasant Gap, PA).

Immunostaining of mouse preimplantation embryos

Immunostaining of "living" mouse preimplantation embryos was performed as previously described [11]. Briefly, cells were incubated in 30 μl drops of M16 medium containing 0.45 μg of Alexa Fluor® 488 or 546 -conjugated 6E2 (final concentration 15 μg/ml), and then they were washed three times in 30 μl drops of M16 medium. All staining steps were carried out at 37°C in a CO_2 incubator for fresh embryos. Cell nuclei were stained with DAPI (Invitrogen), which slowly permeates the living cell membrane and slowly leaks out after washing [24]. For actin and cholesterol staining, embryos were prefixed for 10 minutes at room temperature with 2% paraformaldehyde containing 0.1% glutaraldehyde in 4-(2-hydroxyethyl)-1-piperazineethanesulfonic acid (HEPES) buffered saline (HBS), then permeabilized with 0.01% Triton X-100 in HBS for 10 minutes at room temperature, and blocked with 3% bovine serum albumin. Staining of living embryos and fixed embryos was performed at 37°C and 4°C, respectively. The stained embryos were placed in a microdrop of M16 medium on a glass-bottom dish (IWAKI Glass, Tokyo, Japan), covered with liquid paraffin (NAKALAI TESQUE, Kyoto, Japan), and examined with a LSM510 Zeiss Confocal laser-scanning microscope (Carl Zeiss, Thornwood, NY) and a 40× objective lens so that only the embryo was included in the field of view. For three dimensional (3D) construction, two-dimensional (2D) images were captured as vertical sections (at approximately 2-μm intervals) by using a Z-axis motor, then processed with Zeiss Zen 2009 software (Carl Zeiss), and finally stacked into one picture.

Preparation of BODIPY®FL-MSGb5Cer

MSGb5Cer was purified from human renal cancer cell line ACHN cells by ion-exchange chromatography on DEAE-Sephadex A25 and preparative TLC/TLC blotting according to Taki et al. MSGb5Cer was conjugated to fluorescence reagents with Sphingolipid Ceramide N-deacylase (SCDase) according to the procedure described in the previous report [25]. To prepare lyso-MSGb5Cer, MSGb5Cer was incubated at 37°C for 16 hours with 8 μU of SCDase in 20 μl of 25 mM sodium acetate buffer, pH5.5, containing 0.2% Triton X-100 and 5 mM $CaCl_2$, and the reaction mixture was adsorbed onto an Oasis® MCX cartridge (Waters). The lyso-MSGb5Cer eluted from the cartridge with 5% ammonium hydroxide in methanol was subsequently incubated with BODIPY®FL-C12 (Invitrogen) in 20 μl of the condensation reaction mixture (8 mU SCDase, 25 mM Tris-HCl buffer, pH7.5, 5 mM $MgCl_2$, 0.1% Triton X-100) at 37°C for 16 hours. The reaction mixture was adsorbed to an Oasis MCX cartridge. The methanol eluate was dried, desalted with a DISCOVERY DC-18 cartridge (SUPELCO), and adsorbed to a DISCOVERY DSC-Si cartridge (SUPELCO). The condensed BODIPY®FL-MSGb5Cer product eluted from the cartridge with methanol was analyzed by high performance thin layer chromatography (HPTLC) by using chloroform/methanol/0.02% $CaCl_2$ (5:4:1, v/v) as the developing solvent, and it was viewed by using FLA-7000 (Fuji Film, Tokyo, Japan) (see Figure S3 in additional file 4). BODIPY®FL-GM1 was also prepared in the same manner as described above. MSGb5Cer and GM1 enzymatically conjugated with BODIPY®FL-C12 -fatty acid in ethanol were dissolved in 3.4% non-fatted BSA in Hank's balanced solution and diluted in M16 medium. Two-cell stage embryos were incubated in a drop of the medium for 20 minutes and examined.

Time-lapse imaging

MSGb5Cer was stained by incubating the zygote at 22-26 hours after the hCG injection for 20 minutes in a conventional incubator with Alexa Fluor® 488-conjugated 6E2 Mab and DAPI dissolved in M16 medium. Stained embryos were transferred to a microdrop of M16 medium on a glass-bottom dish covered with

liquid paraffin. During time-laps imaging, samples were placed in a 37°C stage-top incubator (INUBG2-PPZI, Tokai Hit, Japan) with a slow flow of air with 5% CO2 gas and high humidity. An objective heater (INUBG2-PPZI, Tokai Hit, Japan) was also used to maintain the objective temperature at 37°C to reduce temperature gradients within the sample. Time-lapse fluorescence images were taken at 15-minute intervals with a spinning disk confocal scanhead (Yokogawa) attached to an inverted fluorescence microscope (OLYMPUS). Images were captured as vertical sections (approximately 2-μm intervals) by using a Z-axis motor and processed by a deconvolution program using iQ software (Andor). Fluorescence intensity was measured with ImageJ software http://rsb.info.nih.gov/ij/.

Pretreatment of embryos with MbCD

A stock solution of MbCD was prepared in sterile water at 100 mM and diluted with M16 medium. Compacted embryos were preincubated with 0, 0.5, 2.5, 5, and 10 mM MbCD for 15 minutes, and then cultured for 48 hours. The embryos after preincubation with MbCD were immunostained with Alexa Fluor® 488-conjugated 6E2, Alexa Fluor® 546 CTX-B, and ECCD-2/Alexa Fluor® 546 conjugated-rabbit anti-rat IgG to examine the distribution of MSGb5Cer, GM1, and E-cadherin, respectively.

Embryo culture in the presence of anti-MSGb5Cer Mab

Two-cell stage embryos were cultured for 48 hours in M16 medium containing 100 μg/ml of anti-MSGb5Cer Mab 6E2, ECCD-2, or 15B2. ECCD-2 was used as a control Mab that binds to mouse embryos. 15B2 was used as a control Mab subclass-matched to 6E2 that do not binds to mouse embryos. The aliquots of embryos after culture for 2 hours in the presence of 6E2 or 15B2 were fixed and immunostained with Alexa Fluor® 633 phalloidin and ECCD-2/Alexa Fluor® 546 Rabbit Anti-rat IgG to examine the distribution of F-actin and E-cadherin, respectively.

Pretreatment of embryos with CCD

A stock solution of CCD was prepared in DMSO at 2 mg/ml and diluted with M16 medium. Two-cell stage embryos were preincubated for 30 minutes at 37°C with 0, 0.2, and 2 μg/ml of CCD in a CO_2 incubator. After washing with M16 medium, the embryos were immunostained for 1 hour with Alexa Fluor® 488-conjugated 6E2.

Additional material

Additional file 1: MSGb5Cer accumulates at the interface during cytokinesis. 6E2 stained cells were imaged by confocal microscopy during mitosis. Frames were taken every 15 minutes and are displayed at 2 frames per second.

Additional file 2: The data of blastocysts culture in the presence of 100 μg/ml of 6E2.

Additional file 3: Mating scheme used to generate embryos lacking E-cadherin.

Additional file 4: HPTLC showing the preparation of BODIPY®-FL-GM1 and -MSGb5Cer.

List of abbreviations

GSL: Glycosphingolipid; MSGb5Cer: MonosialylGb5ceramide; MbCD: Methyl-beta-cyclodextrin; CCD: Cytochalasin D; Mab: Monoclonal antibody; SSEA-4: Stage-specific embryonic antigen-4; CTX-B: Cholera toxin B subunit; hCG: human chorionic gonadotropin; HEPES: 4-(2-hydroxyethyl)-1-piperazineethanesulfonic acid; HBS: HEPES buffered saline; HPTLC: high performance thin layer chromatography; SCDase: Sphingolipid Ceramide N-deacylase; DIC: differential interference contrast.

Acknowledgements

This work was supported by Health and Labour Sciences Research Grants (the 3rd term comprehensive 10-year-strategy for cancer control H22-011) from the Ministry of Health, Labour and Welfare of Japan. This work was also supported by CREST of Japan Science and Technology Agency, a grant from the Japan Health Sciences Foundation for Research on Publicly Essential Drugs and Medical Devices (KHA1002). B.S is JSPS research fellow.

Author details

[1]Department of Pediatric Hematology and Oncology Research, National Research Institute for Child Health and Development, 2-10-1 Okura, Setagaya-ku, Tokyo 157-8535, Japan. [2]Department of Reproductive Biology, National Research Institute for Child Health and Development, 2-10-1 Okura, Setagaya-ku, Tokyo 157-8535, Japan. [3]Department of Bioscience and Biotechnology, Graduate School of Bioresource and Bioenvironmental Sciences, Kyushu University, Hakozaki 6-10-1, Higashi-ku, Fukuoka 812-8581, Japan. [4]Department of Anatomy and Developmental Biology, Inohana 1-8-1, Chuo-ku, Graduate School of Medicine, Chiba University, Chiba 260-8670, Japan.

Authors' contributions

BS designed and carried out most of experiments and drafted the manuscript. YUK, KT and NK designed the experiments and edited the manuscript. KM, HA, JF and AU helped conceive the experiments and commented on the manuscripts. NO and MI helped in the preparation of fluorescence labeled-glycosphingolipid. JF and NK obtained funding. All authors read and approved the final manuscripts.

Received: 18 November 2010 Accepted: 14 April 2011
Published: 14 April 2011

References

1. Albertson R, Riggs B, Sullivan W: **Membrane traffic: a driving force in cytokinesis.** *Trends Cell Biol* 2005, **15(2)**:92-101.
2. Burgess DR: **Cytokinesis and the establishment of early embryonic cell polarity.** *Biochem Soc Trans* 2008, **36(Pt 3)**:384-386.
3. Bauer T, Motosugi N, Miura K, Sabe H, Hiiragi T: **Dynamic rearrangement of surface proteins is essential for cytokinesis.** *Genesis* 2008, **46(3)**:152-162.
4. Vestweber D, Gossler A, Boller K, Kemler R: **Expression and distribution of cell adhesion molecule uvomorulin in mouse preimplantation embryos.** *Dev Biol* 1987, **124(2)**:451-456.
5. Fleming TP, Javed Q, Hay M: **Epithelial differentiation and intercellular junction formation in the mouse early embryo.** *Dev Suppl* 1992, 105-112.
6. Fleming TP, Sheth B, Fesenko I: **Cell adhesion in the preimplantation mammalian embryo and its role in trophectoderm differentiation and blastocyst morphogenesis.** *Front Biosci* 2001, **6**:D1000-7.
7. Simons K, Ikonen E: **Functional rafts in cell membranes.** *Nature* 1997, **387(6633)**:569-572.
8. Lingwood D, Simons K: **Lipid rafts as a membrane-organizing principle.** *Science* 2010, **327(5961)**:46-50.

9. Ng MM, Chang F, Burgess DR: **Movement of membrane domains and requirement of membrane signaling molecules for cytokinesis.** *Dev Cell* 2005, **9(6)**:781-790.
10. Comiskey M, Warner CM: **Spatio-temporal localization of membrane lipid rafts in mouse oocytes and cleaving preimplantation embryos.** *Dev Biol* 2007, **303(2)**:727-739.
11. Sato B, Katagiri YU, Miyado K, Akutsu H, Miyagawa Y, Horiuchi Y, Nakajima H, Okita H, Umezawa A, Hata J, Fujimoto J, Toshimori K, Kiyokawa N: **Preferential localization of SSEA-4 in interfaces between blastomeres of mouse preimplantaion embryos.** *Biochem Biophys Res Commun* 2007, **364(4)**:838-843.
12. Van Slambrouck S, Hilkens J, Steelant WF: **Ether lipid 1-O-octadecyl-2-O-methyl-3-glycero-phosphocholine inhibits cell-cell adhesion through translocation and clustering of E-cadherin and episialin in membrane microdomains.** *Oncol Rep* 2008, **19(1)**:123-128.
13. Ilangumaran S, Hoessli DC: **Effects of cholesterol depletion by cyclodextrin on the sphingolipid microdomains of the plasma membrane.** *Biochem J* 1998, **335(Pt 2)**:433.
14. Brown DA: **Isolation and use of rafts.** *Curr Protoc Immunol* 2002, Chapter 11:Unit 11.10.
15. Keller P, Simons K: **Cholesterol is required for surface transport of influenza virus hemagglutinin.** *J Cell Biol* 1998, **140(6)**:1357-1367.
16. Pike LJ: **Lipid rafts: heterogeneity on the high seas.** *Biochem J* 2004, **378(Pt 2)**:281-292.
17. Katsumata O, Kimura T, Nagatsuka Y, Hirabayashi Y, Sugiya H, Furuyama S, Yanagishita M, Hara-Yokoyama M: **Charge-based separation of detergent-resistant membranes of mouse splenic B cells.** *Biochem Biophys Res Commun* 2004, **319(3)**:826-831.
18. Lingwood D, Kaiser HJ, Levental I, Simons K: **Lipid rafts as functional heterogeneity in cell membranes.** *Biochem Soc Trans* 2009, **37(Pt 5)**:955-960.
19. Alford LM, Ng MM, Burgess DR: **Cell polarity emerges at first cleavage in sea urchin embryos.** *Dev Biol* 2009, **330(1)**:12-20.
20. Riethmacher D, Brinkmann V, Birchmeier C: **A targeted mutation in the mouse E-cadherin gene results in defective preimplantation development.** *Proc Natl Acad Sci USA* 1995, **92(3)**:855-859.
21. De Vries WN, Evsikov AV, Haac BE, Fancher KS, Holbrook AE, Kemler R, Solter D, Knowles BB: **Maternal beta-catenin and E-cadherin in mouse development.** *Development* 2004, **131(18)**:4435-4445.
22. Boussadia O, Kutsch S, Hierholzer A, Delmas V, Kemler R: **E-cadherin is a survival factor for the lactating mouse mammary gland.** *Mech Dev* 2002, **115(1-2)**:53-62.
23. Nakano T, Umezawa A, Abe H, Suzuki N, Yamada T, Nozawa S, Hata J: **A monoclonal antibody that specifically reacts with human embryonal carcinomas, spermatogonia and oocytes is able to induce human EC cell death.** *Differentiation* 1995, **58(3)**:233-240.
24. Miyado K, Yoshida K, Yamagata K, Sakakibara K, Okabe M, Wang X, Miyamoto K, Akutsu H, Kondo T, Takahashi Y, Ban T, Ito C, Toshimori K, Nakamura A, Ito M, Miyado M, Mekada E, Umezawa A: **The fusing ability of sperm is bestowed by CD9-containing vesicles released from eggs in mice.** *Proc Natl Acad Sci USA* 2008, **105(35)**:12921-12926.
25. Furusato M, Sueyoshi N, Mitsutake S, Sakaguchi K, Kita K, Okino N, Ichinose S, Omori A, Ito M: **Molecular cloning and characterization of sphingolipid ceramide N-deacylase from a marine bacterium, Shewanella alga G8.** *J Biol Chem* 2002, **277(19)**:17300-17307.

doi:10.1186/1471-213X-11-22
Cite this article as: Sato *et al.*: Lipid rafts enriched in monosialylGb5Cer carrying the stage-specific embryonic antigen-4 epitope are involved in development of mouse preimplantation embryos at cleavage stage. *BMC Developmental Biology* 2011 11:22.

bjh research paper

Clinical significance of early T-cell precursor acute lymphoblastic leukaemia: results of the Tokyo Children's Cancer Study Group Study L99-15

Takeshi Inukai,[1] Nobutaka Kiyokawa,[2] Dario Campana,[3,4] Elaine Coustan-Smith,[3,4] Akira Kikuchi,[5] Miyuki Kobayashi,[6] Hiroyuki Takahashi,[7] Katsuyoshi Koh,[5] Atsushi Manabe,[8] Masaaki Kumagai,[9] Koichiro Ikuta,[10] Yasuhide Hayashi,[11] Masahiro Tsuchida,[12] Kanji Sugita[1] and Akira Ohara[13]

[1]Department of Paediatrics, School of Medicine, University of Yamanashi, Yamanashi, [2]Department of Developmental Biology, National Research Institute for Child Health and Development, Tokyo, Japan, [3]Department of Oncology, St. Jude Children's Research Hospital, Memphis, TN, USA, [4]Department of Paediatrics, National University of Singapore, Singapore, [5]Department of Hematology/Oncology, Saitama Children's Medical Centre, Saitama, [6]Department of Paediatrics, Graduate School of Medicine, University of Tokyo, Tokyo, [7]Department of Paediatrics, Saiseikai Yokohama City Nanbu Hospital, Yokohama, [8]Department of Paediatrics, St. Luke's International Hospital, [9]Department of Paediatric Hematology/Oncology, National Centre for Child Health and Development, Tokyo, [10]Department of Paediatrics, School of Medicine, Yokohama City University, Yokohama, [11]Department of Hematology/Oncology, Gunma Children's Hospital, Maebashi, [12]Department of Paediatric Hematology and Oncology, Ibaraki Children's Hospital, Mito, and [13]First Department of Paediatrics, Toho University, Tokyo, Japan

Received 6 August 2011; accepted for publication 27 October 2011

Correspondence: Takeshi Inukai, Department of Paediatrics, School of Medicine, University of Yamanashi, Yamanashi, Japan.
E-mail: tinukai@yamanashi.ac.jp

Summary

Early T-cell precursor acute lymphoblastic leukaemia (ETP-ALL) is a recently identified subtype of T-ALL with distinctive gene expression and cell marker profiles, poor response to chemotherapy and a very high risk of relapse. We determined the reliability of restricted panel of cell markers to identify EPT-ALL using a previously classified cohort. Then, we applied the cell marker profile that best discriminated ETP-ALL to a cohort of 91 patients with T-ALL enrolled in the Tokyo Children's Cancer Study Group L99-15 study, which included allogeneic stem cell transplantation (allo-SCT) for patients with poor prednisone response. Five of the 91 patients (5·5%) met the ETP-ALL criteria. There were no significant differences in presenting clinical features between these and the remaining 86 patients. Response to early remission induction therapy was inferior in ETP-ALL as compared with T-ALL. The ETP-ALL subgroup showed a significantly poorer event-free survival (4-year rate; 40%) than the T-ALL subgroup (70%, $P = 0·014$). Of note, three of four relapsed ETP-ALL patients survived after allo-SCT, indicating that allo-SCT can be effective for this drug-resistant subtype of T-ALL.

Keywords: acute lymphoblastic leukaemia, childhood, Early T-cell precursor, cell marker profile, allogeneic stem cell transplantation.

In approximately 15% of patients with childhood acute lymphoblastic leukaemia (ALL) leukaemic lymphoblasts have an immunophenotype corresponding to immature T cells (Pullen *et al*, 1999). Although the prognosis of childhood T-cell acute lymphoblastic leukaemia (T-ALL) has dramatically improved (Goldberg *et al*, 2003; Pui *et al*, 2009), patients with

First published online 30 November 2011
doi:10.1111/j.1365-2141.2011.08955.x

T-ALL continue to have an increased risk of relapse compared to those with B-precursor ALL (Pullen *et al*, 1999; Pui & Evans, 2006; Pui *et al*, 2008). In childhood B-precursor ALL patients, clinical presenting features (age and leucocyte count at diagnosis) and chromosomal translocations predict therapeutic outcome, and have been used for risk-specific adjustments in therapeutic intensity (Pui & Evans, 2006; Pui *et al*, 2008). Much effort has been put into identifying prognostically relevant clinical and biological features for childhood T-ALL (Schneider *et al*, 2000; Weng *et al*, 2004; Gottardo *et al*, 2007; Winter *et al*, 2007; Dalmazzo *et al*, 2009; Karrman *et al*, 2009; Attarbaschi *et al*, 2010; Cleaver *et al*, 2010; Zuurbier *et al*, 2010), but none is sufficiently discriminatory to be used for treatment stratification in contemporary protocols.

A recent study identified a distinct biological subtype of T-ALL, early T-cell precursor ALL (ETP-ALL) (Coustan-Smith *et al*, 2009), characterized by a gene expression profile recapitulating that of normal ETP cells, a subpopulation of thymocytes that retain multi-lineage differentiation potential (Bell & Bhandoola, 2008). ETP-ALL can be recognized by a distinctive cell surface antigen profile: lack of CD1a and CD8, weak CD5, and expression of one or more myeloid- or stem cell-related antigens. Notably, ETP-ALL was associated with an inferior clearance of leukaemia cells after the first phase of remission induction therapy and extremely poor event-free and overall survival in patients treated on intensified chemotherapeutic protocols both at the St Jude Children's Research Hospital and the Associazione Italiana Ematologia Oncologia Pediatrica (AIEOP) (Coustan-Smith *et al*, 2009).

To verify the impact of prognostic significance of ETP-ALL, we studied patients with T-ALL in the Tokyo Children's Cancer Study Group (TCCSG) L99-15 study (Manabe *et al*, 2008). Because the cell marker panel used in this multicentre protocol did not include all of the markers required for diagnosis of ETP-ALL, we first establish a scoring system based on a more limited panel which could effectively differentiate ETP-ALL from T-ALL in a previously reported cohort (Coustan-Smith *et al*, 2009). Using this scoring system, we retrospectively identified patients with ETP-ALL in the TCCSG L99-15 study, and determined their presenting features, response to chemotherapy, and rates of relapse.

Materials and methods

Patients

Seven hundred and seventy patients (1–18 years of age) diagnosed with ALL were consecutively enrolled in the TCCSG L99-15 study from February 1999 to July 2003 (Manabe *et al*, 2008). The diagnosis of ALL was based on morphological, biochemical, and flow cytometric features of leukaemia cells. Flow cytometric analysis was performed in institutional or commercial laboratories, and the results were reviewed by members of the TCCSG diagnostic committee. Among 754 eligible ALL patients, 91 patients were diagnosed as T-ALL based on the expression of CD7 and at least one other T-cell marker on leukaemia cells with negative myeloperoxidase reaction (<3%); 90 patients were initially enrolled as T-ALL (Manabe *et al*, 2008) and one patient whose initial diagnosis was unclassified leukaemia was retrospectively diagnosed as T-ALL. The study was approved by the institutional review boards of the participating institutions or the equivalent organization with written informed consent from the parents or guardians of the patients.

For testing the usefulness of the scoring system, previously reported data of flow cytometric analyses of T-ALL patients from the St Jude Children's Research Hospital (St Jude cohort) were studied (Coustan-Smith *et al*, 2009). In the St Jude cohort, based on the findings of the flow cytometric analysis and gene expression profile, 17 patients were diagnosed as having ETP-ALL and 122 patients as having typical T-ALL (Coustan-Smith *et al*, 2009).

Treatment protocol

Details of the treatment regimen have been previously reported (Manabe *et al*, 2008). After 1 week oral administration of prednisolone (60 mg/m^2), patients were stratified into three treatment subgroups: those with $<0{\cdot}001 \times 10^9$ blasts/l in peripheral blood were categorized as intermediate risk (IR), those with $0{\cdot}001$–$0{\cdot}999 \times 10^9$ blasts/l as high risk (HR), and those with $\geq 1{\cdot}0 \times 10^9$ blasts/l were categorized as HR-SCT, and regarded as candidates for allogeneic stem cell transplantation (allo-SCT) in first remission. The determination of blasts in peripheral blood and bone marrow was done by microscopic evaluation at each institution. Patients in all three of the treatment subgroups underwent identical induction therapy composed of prednisolone, vincristine, cyclophosphamide, daunorubicin and asparaginase with triple intrathecal injection therapy. IR patients were randomized to receive high-dose cytarabine (2 g/m^2) or cytarabine (75 g/m^2) plus cyclophosphamide and 6-mercaptopurine in the post-remission induction intensification phase. HR and HR-SCT patients were treated with high-dose cytarabine in the post-remission induction intensification phase. Patients with an initial white blood cell (WBC) count $\geq 100 \times 10^9$ blasts/l in the IR and HR subgroups received prophylactic cranial irradiation (12 Gy for patients aged 1–6 years, and 18 Gy for patients aged 7 years and older). HR-SCT patients underwent allo-SCT in first remission; the recommended timing for SCT was after four or five courses of intensification therapy (corresponding to 7–8 months after diagnosis).

Statistical analysis

Clinical features of patients were compared using the chi-square test, and blast counts of bone marrow and peripheral blood were compared using the Mann–Whitney test. To compare cell surface antigen expression levels between patients with ETP-ALL and patients with typical T-ALL in

the St Jude cohort, we performed either the student's *t*-test or the *t*-test for unequal variances based on the *F* value for sample variances. The duration of event-free survival was defined as the time from the initiation of therapy to either treatment failure (relapse, death, or diagnosis of secondary cancer) or to the last day when the patient was confirmed to be in remission. The probabilities of event-free survival and overall survival were estimated by the Kaplan–Meier analysis, and were tested for significance using log-rank test. For univariate and multivariate analysis, the Cox proportional hazards model was employed to assess risk factors on even-free survival. *P* values <0·05 were considered statistically significant.

Results

Development of an ETP-ALL scoring system

ETP-ALL shows a distinctive immature immunophenotype characterized by lack of CD1a and CD8 expression, weak CD5 expression with <75% positive blasts, and expression of one or more of the following myeloid or stem cell antigens on at least 25% of lymphoblasts: CD117, CD34, HLA-DR, CD13, CD33, CD11b and/or CD65 (Coustan-Smith *et al*, 2009). Among the T-ALL patients enrolled in the TCCSGL99-15 study, data for some of the markers were only available in a limited group of patients (e.g. CD1a and CD11b were available for 67% and 7%

(A)

Scoring system based on 6 marker expression		
Score	−1	+1
CD5	≥5%	<75%
CD8	≥5%	<5%
CD13		≥25%
CD33		≥25%
CD34		≥25%
HLA-DR		≥25%

(C)

Scoring system based on 11 marker expression				
Score	−2	−1	+1	+2
CD5	≥75%			<75%
CD8	≥5%			<5%
CD13			≥25%	≥75%
CD33			≥25%	≥75%
CD34			≥25%	≥75%
HLA-DR			≥25%	≥75%
CD2		≥75%	<20%	
CD3		≥75%	<20%	
CD4		≥75%	<20%	
CD10		≥75%	<20%	
CD56			≥20%	

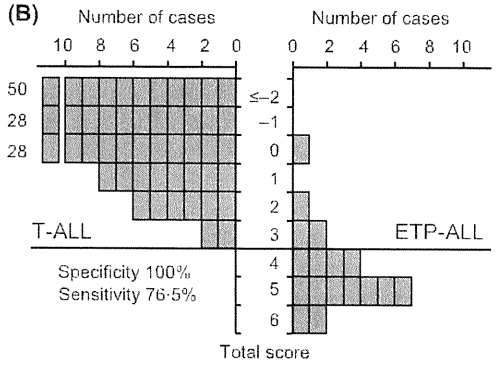

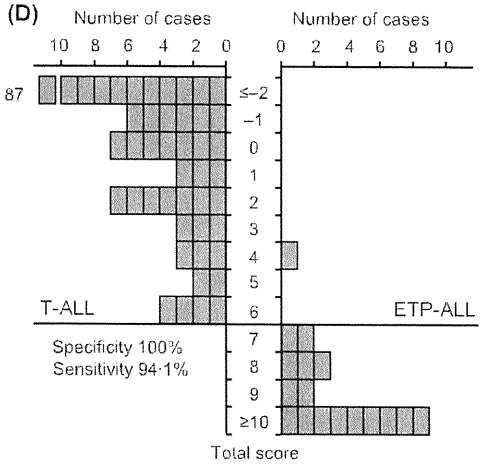

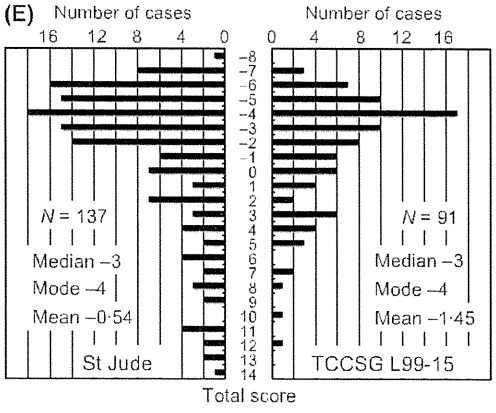

Fig 1. Establishment of a scoring system for immunophenotypical diagnosis of early T-cell precursor acute lymphoblastic leukaemia (ETP-ALL). (A) Scoring system based on the expression of six cell surface markers. (B) Distribution of total score of 6-marker expression in 17 ETP-ALL cases (right) and 122 T-ALL cases (left) of the St Jude cohort. (C) Scoring system based on the expression of 11 markers. (D) Distribution of total score of 11-marker expression in ETP-ALL patients (right) and T-ALL patients (left) of the St Jude cohort. (E) Distribution of total score of 11-marker expression in 139 T-ALL cases of the St Jude cohort (left) and 91 T-ALL cases of the TCCSG L99-15 study (right).

Table I. Profiling of cell surface marker expression of ETP-ALL patients.

Score	CD1a	CD2	CD3	CD4	CD5	CD7	CD8	CD10	CD13	CD33	CD34	CD56	HLA-DR	Others
12	NT	3·4	12·7	1·3	1·9	68·0	1·2	1·0	67·7	61·9	61·9	0·7	52·1	cyCD3$^+$
10	0·4	2·5	1·6	0·5	26·2	99·0	2·2	1·4	92·4	3·4	0·8	0·3	4·4	
8	0·5	93·8	1·7	NT	4·1	97·6	NT	0·5	93·5	6·2	99·2	7·4	37·2	CD11b$^+$
7	0·8	11·7	2·7	18·1	71·5	96·7	1·9	66·2	17·5	0·3	16·8	NT	1·3	
7	0·2	78·8	0·3	0·6	1·1	95·7	2·3	72·0	81·9	12·6	2·4	NT	3·2	

NT, not tested.

of patients respectively) or not available at all (CD65 and CD117). Thus, we devised a scoring system based on the expression of six markers; CD5, CD8, CD13, CD33, CD34 and HLA-DR (Fig 1A) and applied it to the St Jude cohort, which included 17 ETP-ALL and 122 non-ETP T-ALL patients (Coustan-Smith *et al*, 2009). As shown in Fig 1B, the total score for all of the 122 typical T-ALL cases was a maximum of three, while it was four or more in 13 of the 17 ETP-ALL cases. Thus, the specificity was 100%, and the sensitivity 77%.

We next focused on the expression levels of the other antigens that were originally not included in the definition of ETP-ALL. In the St Jude cohort (Coustan-Smith *et al*, 2009), the expression levels of CD2 ($P < 0·01$, *t*-test), sCD3 ($P < 0·01$), CD4 ($P < 0·01$), and CD10 ($P = 0·035$) were significantly lower in ETP-ALL than in typical T-ALL, whereas the expression level of CD56 was significantly higher ($P = 0·018$) in ETP-ALL than in typical T-ALL. Thus, we established a second scoring system by the combination of these five additional markers (CD2, sCD3, CD4, CD10 and CD56) with the six used in the first analysis (CD5, CD8, CD13, CD33, CD34 and HLA-DR) (Fig 1C). When we applied this scoring system to the St Jude cohort, the total score in typical T-ALL patients was always six and lower, while it was seven or more in 16 of the 17 ETP-ALL patients (Fig 1D); specificity and sensitivity were 100% and 94%, respectively.

Application of scoring system to TCCSG L99-15 study

We applied the scoring system that included the 11 markers to the TCCSG L99-15 cohort (Fig 1E). In the TCCSG L99-15 study, median and mode of total score were -3 and -4 respectively, identical to those in the St Jude cohort. Among 91 T-ALL cases of the TCCSG L99-15 study, 5 (5·5%) had a score ≥7. The cell surface antigen expression profile of these five patients is summarized in Table I. Four patients showed typical ETP-ALL immunophenotype with negative CD1a expression; the remaining patient had no CD1a expression data but their cells had an immunophenotype with the highest total score of 12. The 86 patients (94·5%) whose total score were 6 and lower (Fig 1E) were considered as having non-ETP T-ALL. Among these 86 patients, however, there were 13 whose immunophenotype showed marginal patterns with a score of 3–6 (Table SI).

Clinical features and early treatment response of ETP-ALL

Table II summarizes the patient characteristics of ETP-ALL ($n = 5$) and T-ALL ($n = 86$). Distributions of gender, higher initial WBC count, age, National Cancer Institute (NCI) risk group, mediastinal mass, French-American-British

Table II. Demographic characteristics of the patients.

		T-ALL	ETP-ALL	χ^2-test
		N = 86	*N* = 5	*P*
Sex	Male	67	2	0·089
	Female	19	3	
WBC	≥100 × 10^9/l	42 (48·8%)	1 (20%)	0·36
Age	≥10 Years old	39 (45·3%)	3 (60%)	0·66
NCI risk group	Standard	14	1	1·0
	High	72	4	
Mediastinal mass	Yes	51 (59·3%)	3 (60%)	1·0
FAB classification	L1	59	2	0·32
	L2	25	3	
CNS involvement	Yes	3 (3·5%)	0 (0%)	1·0
Treatment subgroup	IR	22	1	
	HR	33	0	
	HR-SCT	31	4	
	HR-SCT%	36·0%	80%	0·070
Remission failure	Yes	4/85 (4·7%)	0/5 (0%)	1·0
Relapse	BM	15	4	
	CNS	2	0	
	Thymus	1	0	
	BM + thymus	2	0	
	Unknown	2	0	
SCT	Yes	42/85 (49·4%)	5/5 (100%)	0·057
Status at SCT	CR1	28	2	
	CR2	3	2	
	CR3	1	0	
	Failure	1	0	
	Rel1	3	1	
	Rel2	1	0	
	Unknown	5	0	

WBC, white blood cell count; NCI, National Cancer Institute; FAB, French-American-British; CNS, central nervous system; IR, intermediate risk; HR, high risk; SCT, allogeneic stem-cell transplantation; BM, bone marrow; CR1, first remission; CR2, second remission; CR3, third remission; Rel1, first relapse; Rel2, second relapse.

classification, and central nervous system involvement were not significantly different between the two groups. Clinical features at diagnosis of 13 borderline patients were similar to those of remaining 73 T-ALL patients (data not shown). Karyotypic analysis showed that two patients with ETP-ALL had +4 abnormality, which was not observed in the remaining patients (data not shown). Blast counts in peripheral blood (Fig 2A) and bone marrow (Fig 2B) at diagnosis were not significantly different between the two groups.

Although peripheral blast counts after 1 week monotherapy with prednisolone (Fig 2C) were similar between patients with ETP-ALL and T-ALL, bone marrow blast counts on day 14 remission induction therapy (Fig 2D) and blast counts in peripheral blood on day 15 (Fig 2E) were higher in patients with EPT-ALL ($P = 0{\cdot}057$ and $P = 0{\cdot}004$ by Mann–Whitney test respectively). Interestingly, among the 13 phenotypically borderline cases, blast counts in peripheral blood on day 8 and those in bone marrow on day 14 were significantly higher than those in remaining T-ALL patients (Fig S1).

Treatment outcome of ETP-ALL

Induction failures were observed in four of the patients with T-ALL but in none of those with ETP-ALL (Table II). Relapse occurred in 22 of the 82 (26·8%) patients with T-ALL who achieve remission and in four of the five patients with ETP-ALL. Due to HR-SCT classification and/or relapse, allo-SCT was performed in 41 patients (49·4%) with T-ALL and all five patients with ETP-ALL. With a median follow-up of 5·3 years, the estimated 4-year rate of event-free survival (Fig 3A) was 70·9% [95% confidence interval (CI), 61·1–80·7] for patients with T-ALL as compared to 40·0% (95% CI, 0–82·9) for those with ETP-ALL ($P = 0{\cdot}014$ by log-rank test). In a univariate analysis, ETP-ALL was a significant adverse risk factor for relapse ($P = 0{\cdot}048$). In a multivariate analysis including EPT-ALL, responses to prednisolone, NCI risk group, therapeutic subgroup, and gender as category terms, ETP-ALL was significant risk factor for relapse ($P = 0{\cdot}014$). Among the five patients with ETP-ALL (Table III), three patients who relapsed

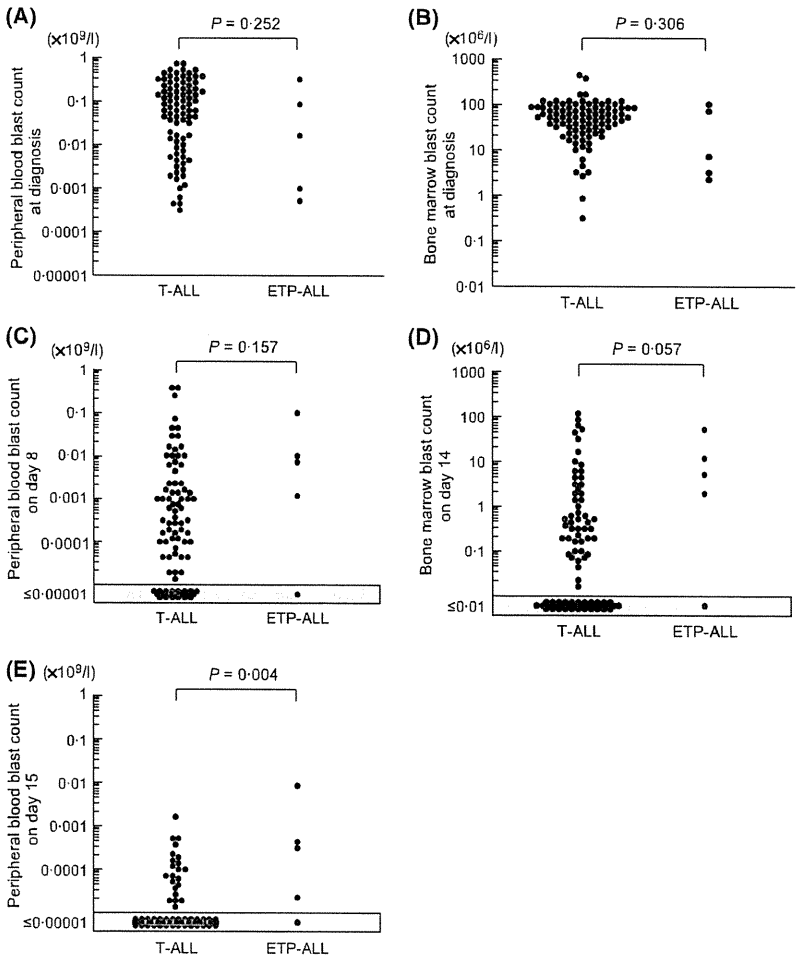

Fig 2. Comparison of blast counts in the patients having ETP-ALL with those in the patients having T-ALL. Blast counts in (A) peripheral blood at diagnosis, (B) bone marrow at diagnosis, (C) peripheral blood on day 8, (D) bone marrow on day 14, and (E) peripheral blood on day 15 were compared by Mann–Whitney analysis, and each P value is indicated at the top of figures.

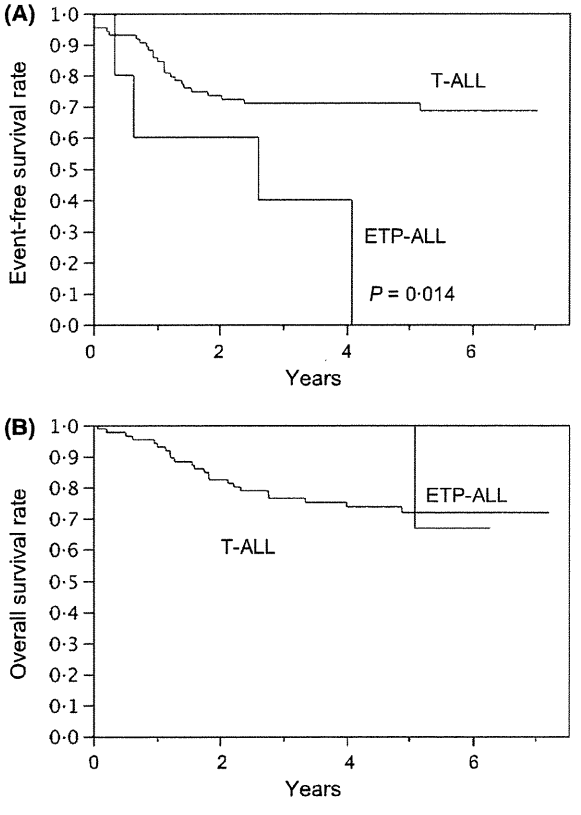

Fig 3. Kaplan–Meier plots of (A) event-free survival and (B) overall survival of the patients with ETP-ALL and T-ALL patients.

3, 7 and 48 months from diagnosis remained in second remission for 64, 67 and 8 months after allo-SCT. Thus, four of the five patients with ETP-ALL are alive in first (one patient) or second remission (three patients) (Fig 3B). Due to poor prednisolone response, 8 of the 13 borderline patients (62%) underwent allo-SCT in first remission at 6–9 months (median 7·5 months) after diagnosis, and all eight patients are alive in first remission (Table SII). As a result, the event-free survival of 13 borderline patients was similar (76·9%; 95% CI, 54·0–99·8) to that of the remaining T-ALL patients and significantly better than that of bona fide ETP-ALL patients ($P = 0·031$, log-rank test).

Discussion

As cure rates for children with ALL approach 90%, it has become ever more important to identify small subgroup of patients who are resistant to modern intensive chemotherapy. Among patients with T-ALL, reliable prognostic indicators have been lacking (Pui & Evans, 2006; Pui *et al*, 2008). Reportedly, however, patients with ETP-ALL have a particularly poor response to chemotherapy (Coustan-Smith *et al*, 2009) suggesting that alternative treatment approaches are needed for this leukaemia subtype. In the present study, we sought to determine the prevalence of ETP-ALL among patients with T-ALL enrolled in our TCCSG L99-15 study and assess their treatment outcome. Because of the limited panel of markers tested at diagnosis, we first devised a scoring system that allowed the identification of ETP-ALL among a previously reported cohort with 100% specificity and 94% sensitivity. The five patients with ETP-ALL identified among those enrolled in the TCCSG L99-15 study had a significantly poorer response to initial therapy as indicated by higher blast counts of peripheral blood at day 15, consistent with the previous findings of higher minimal residual disease levels observed among patients with ETP-ALL in both St Jude and AIEOP cohorts (Coustan-Smith *et al*, 2009). The event-free survival of ETP-ALL patients was significantly inferior in comparison with that of T-ALL patients. Four of the five patients with ETP-ALL enrolled in our study relapsed, confirming the dismal response to therapy of this T-ALL subtype. However, three of these four patients are alive in second remission after receiving allo-SCT, suggesting that allo-SCT should be considered as a frontline therapy for patients with ETP-ALL in first remission.

The prevalence of ETP-ALL in our study (5·5%) was lower than that determined in the St Jude's (12·2%) and AIEOP (13·0%) cohorts (Coustan-Smith *et al*, 2009). One possibility is that some cases with ETP-ALL may have been misclassified as typical T-ALL owing to the limited panel of markers used. Thus, we examined the borderline cases where patient immunophenotype showed marginal patterns, and found that

Table III. Clinical features of stem-cell transplantation in patients with ETP-ALL.

	SCT				Relapse		Final outcome		
Score	Status	Donor	Source	Time from diagnosis (months)	Site	Time from diagnosis (months)	Status	Survival	Time from diagnosis (months)
12	CR2	Unrelated	CB	6	BM	3	CR2	Alive	70
10	CR1	Sibling	BM	8	BM	31	Rel3	Dead	58
8	CR1	Unrelated	BM	8	No		CR1	Alive	31
7	Rel1	Sibling	PBSC	8	BM	7	CR2	Alive	75
7	CR2	Unrelated	BM	53	BM	48	CR2	Alive	61

SCT, allogeneic stem cell transplantation; CB, cord blood cell; BM, bone marrow; PBSC, peripheral blood stem cell; CR1, first remission; CR2, second remission; Rel1, first relapse; Rel3, third relapse.

almost two thirds of these borderline patients underwent allo-SCT early in first remission because of poor responses to prednisolone and early phase of induction therapy. Of note, all of these patients are alive in first remission, and the resultant event-free survival of the borderline patients was significantly better than that of bona fide ETP-ALL patients. These observations suggest that allo-SCT improves final outcome of the borderline subgroup even if some ETP-ALL patients are included. This seems to be consistent with the previous findings by the Berlin-Frankfürt-Münster group, which reported that allo-SCT was superior to chemotherapy alone in high-risk childhood T-ALL (Schrauder *et al*, 2006). Another possible explanation is that some cases may have been classified as acute myeloid leukaemia because of the expression of multiple myeloid markers and therefore were not enrolled in TCCSG L99-15. The possibility of differences in prevalence due to the different ancestry of the various cohorts should also be considered.

Acknowledgements

The authors would like to thank Mrs Kaori Itagaki for preparing the manuscript.

Authorship

T.I., N.K. and D.C. analysed data and wrote the paper. E.C., A.K., M.K. and H.T. analysed data. K.K., A.M., M.K., K.I., Y.H., M.T. and K.S. designed the research study. A.O. designed the research study, analysed data, and wrote the paper.

Conflict of Interest

These authors declare no conflict of interest.

Source of funding

This study was supported by a grant from the Children's Cancer Association of Japan.

Supporting Information

Additional Supporting Information may be found in the online version of this article:

Fig S1. Comparison of blast counts between borderline patients and remaining T-ALL patients.

Table SI. Profiling of cell surface marker expression of borderline patients.

Table SII. Clinical features of stem-cell transplantation in borderline patients.

Please note: Wiley-Blackwell are not responsible for the content or functionality of any supporting materials supplied by the authors. Any queries (other than missing material) should be directed to the corresponding author for the article.

References

Attarbaschi, A., Pisecker, M., Inthal, A., Mann, G., Janousek, D., Dworzak, M., Pötschger, U., Ullmann, R., Schrappe, M., Gadner, H., Haas, O.A., Panzer-Grümayer, R. & Strehl, S.; Austrian Berlin-Frankfurt-Münster (BFM) Study Group (2010) Prognostic relevance of TLX3 (HOX11L2) expression in childhood T-cell acute lymphoblastic leukaemia treated with Berlin-Frankfurt-Münster (BFM) protocols containing early and late re-intensification elements. *British Journal of Haematology*, **148,** 293–300.

Bell, J.J. & Bhandoola, A. (2008) The earliest thymic progenitors for T cells possess myeloid lineage potential. *Nature*, **452,** 764–767.

Cleaver, A.L., Beesley, A.H., Firth, M.J., Sturges, N.C., O'Leary, R.A., Hunger, S.P., Baker, D.L. & Kees, U.R. (2010) Gene-based outcome prediction in multiple cohorts of pediatric T-cell acute lymphoblastic leukemia: a Children's Oncology Group study. *Molecular Cancer*, **9,** 105–116.

Coustan-Smith, E., Mullighan, C.G., Onciu, M., Behm, F.G., Raimondi, S.C., Pei, D., Cheng, C., Su, X., Rubnitz, J.E., Basso, G., Biondi, A., Pui, C.H., Downing, J.R. & Campana, D. (2009) Early T-cell precursor leukaemia: a subtype of very high-risk acute lymphoblastic leukaemia. *Lancet Oncology*, **10,** 147–155.

Dalmazzo, L.F., Jácomo, R.H., Marinato, A.F., Figueiredo-Pontes, L.L., Cunha, R.L., Garcia, A.B., Rego, E.M. & Falcão, R.P. (2009) The presence of CD56/CD16 in T-cell acute lymphoblastic leukaemia correlates with the expression of cytotoxic molecules and is associated with worse response to treatment. *British Journal of Haematology*, **144,** 223–229.

Goldberg, J.M., Silverman, L.B., Levy, D.E., Dalton, V.K., Gelber, R.D., Lehmann, L., Cohen, H.J., Sallan, S.E. & Asselin, B.L. (2003) Childhood T-cell acute lymphoblastic leukemia: the Dana-Farber Cancer Institute acute lymphoblastic leukemia consortium experience. *Journal of Clinical Oncology*, **21,** 3616–3622.

Gottardo, N.G., Hoffmann, K., Beesley, A.H., Freitas, J.R., Firth, M.J., Perera, K.U., de Klerk, N.H., Baker, D.L. & Kees, U.R. (2007) Identification of novel molecular prognostic markers for paediatric T-cell acute lymphoblastic leukaemia. *British Journal of Haematology*, **137,** 319–328.

Karrman, K., Forestier, E., Heyman, M., Andersen, M.K., Autio, K., Blennow, E., Borgström, G., Ehrencrona, H., Golovleva, I., Heim, S., Heinonen, K., Hovland, R., Johannsson, J.H., Kerndrup, G., Nordgren, A., Palmqvist, L. & Johansson, B.; Nordic Society of Pediatric Hematology, Oncology (NOPHO); Swedish Cytogenetic Leukemia Study Group (SCLSG); NOPHO Leukemia Cytogenetic Study Group (NLCSG). (2009) Clinical and cytogenetic features of a population-based consecutive series of 285 pediatric T-cell acute lymphoblastic leukemias: rare T-cell receptor gene rearrangements are associated with poor outcome. *Genes Chromosomes Cancer*, **48,** 795–805.

Manabe, A., Ohara, A., Hasegawa, D., Koh, K., Saito, T., Kiyokawa, N., Kikuchi, A., Takahashi, H., Ikuta, K., Hayashi, Y., Hanada, R. & Tsuchida, M.; Tokyo Children's Cancer Study Group. (2008) Significance of the complete clearance of peripheral blasts after 7 days of prednisolone treatment in children with acute lymphoblastic leukemia: the Tokyo Children's Cancer Study Group Study L99-15. *Haematologica*, **93,** 1155–1160.

Pui, C.H. & Evans, W.E. (2006) Treatment of acute lymphoblastic leukemia. *New England Journal of Medicine*, **354,** 166–178.

Pui, C.H., Robison, L.L. & Look, A.T. (2008) Acute lymphoblastic leukaemia. *Lancet*, **371,** 1030–1043.

Pui, C.H., Campana, D., Pei, D., Bowman, W.P., Sandlund, J.T., Kaste, S.C., Ribeiro, R.C.,